Indian Journal of Science and Technology, Vol 8(18), DOI: 10.17485/ijst/2015/v8i18/67723, August 2015
ISSN (Print) : 0974-6846
ISSN (Online) : 0974-5645

Comparative Assessment on Ramp and Bias Voltage Variations of Closed Loop Interferometric Fiber Optic Gyroscope

T. Sireesha* and K Sreenivasa Ravi

Department of ECM, K. L. University, Guntur District - 522502, Andhra Pradesh, India; sirishatammana@gmail.com, ravi.kavaluri@kluniversity.in

Abstract

Background/Objectives: The main objective of this paper is to perform a comparative discussion in gyro parameters for three cases: (i) V2π (vary) & Vπ/2 (constant), (ii) Vπ/2 (vary) and V2π (constant) and (iii) both V2π and Vπ/2 are varying simultaneously. **Methods/Statistical analysis**: Fibre optic gyroscope has to be operated in closed-loop approach to achieve the inertial-grade-performance. The Closed-Loop Interferometric Fibre Optic Gyroscope (CLIFOG) system depends upon ramp voltage (V2π of IOC) and square-wave biasing signal frequency (f_{bias}). The digital-phase-ramp-function is used as feedback to system and makes gyro to null condition. The biasing signal voltage (Vπ/2) is $1/4^{th}$ of ramp voltage (V2π). If there are any variations in ramp and biasing signal voltages, then it introduces variations in gyro performance. **Results**: The ramp voltage (V2π) and square wave biasing signal voltage (Vπ/2) is increased from 1% to 10%, decreased to 1% to 10% and performed the various tests for three cases. From results, it was noted that: (i) When V2π is varying and Vπ/2 is kept constant, the scale-factor change is increasing as the error in the signal voltage is also increases. (ii) When V2π is kept constant and Vπ/2 is varying, the change in scale-factor is very minute and maintains the scale-factor linearity. (iii) While varying both V2π and Vπ/2 voltages simultaneously, the device is not responding accordingly as the error is increasing and also scale-factor is out of range subsequently. The effects on the CLIFOG system are described with the derived values in terms of bias and scale-factor. The gyro performance is very sensitive with respect to V2π variations and the percentage error is high in gyro output, but very less effect due to Vπ/2 variations when the ramp voltage (V2π) is constant. **Conclusion/Application:** The Closed Loop Interferometric Fiber Optic Gyroscope (CLIFOG) system requires a proper resetting of ramp voltage (V2π) in order to avoid the bias and scale factor instabilities.

Keywords: CLIFOG, Closed Loop Approach, Fiber Optic Gyroscope, Ramp Voltage (V2π), Square Wave bias Voltage (Vπ/2)

1. Introduction

During the middle of 1970s, the advent of the Fiber Optic Gyroscope (FOG) was developed and demonstrated the optical fiber rotation sensor by Vali and Shorthill. Later, in 1968, R.B. Brown from the Navy Laboratory, revolutionized about the concept behind FOG and proposed a fiber optic coil as a rotation sensor. By using the low-loss single mode fiber an optical fiber ring interferometer was demonstrated by Fringes in 1975[1]. Investigation of FOG was made by a number of researchers, developers, universities, industrial laboratories such as McDonnell Douglas, Northrop-Grumman (Litton), Honeywell, Northrop, Singer, Lear Siegler, Martin Marietta, others etc., and this makes the concept of FOG becomes a reality in world-wide development. In the early 1980s, Gyroscope bias errors reduce to 0.01°/hr succeeded in the laboratory.

The development of the FOG has flourished during the past 30 years. There is a gradual improvement in the performance of FOG and is now quite mature and capable of succeeding the most accurate requirements of gyroscope. This tends to a laboratory experiment evolved into the production floors and practical applications such as in navigation, guidance and control of

*Author for correspondence

aircraft, missiles, automobiles, robots and spacecraft. The competing technologies of FOG from mechanical gyroscopes and ring laser gyroscopes[2] are as shown in the Figure 1.

During the 1980s, RLGs started replacing the mechanical gyroscopes which are still the most widely used navigation grade instruments. However RLG is a complex technology challenge as it needs very good quality optical components. It also has a problem of dead zone because of coupling between backscattered light with counter rotating beams[3].

Fiber optic gyro technology has support from the growing fields namely, fiber optic communication and silicon technology. In modern telecommunications, there is a growing importance of fiber optic technology with a significant advances in some specialized areas such as light sources, low loss couplers, fiber polarizer's and integrated optics, which results in miniaturization, better performance and higher reliability[4].

The forecast of the near term gyro technology requirement could be met by fiber optic gyroscopes starting from very low to the higher end applications and RLG will be required for very high end applications where the scale factor accuracy better that 5ppm is required. However based on the available resources our present development is therefore clear: FOG for short and medium range missile applications and RLG for long range missiles and aircraft applications[5].

There are two configurations exist in FOG are: Interferometric Fiber Optic Gyroscopes (IFOGs) and Resonant Fiber Optic Gyroscopes (RFOG)[6]. The RFOG is used in research stages and gyroscope performance

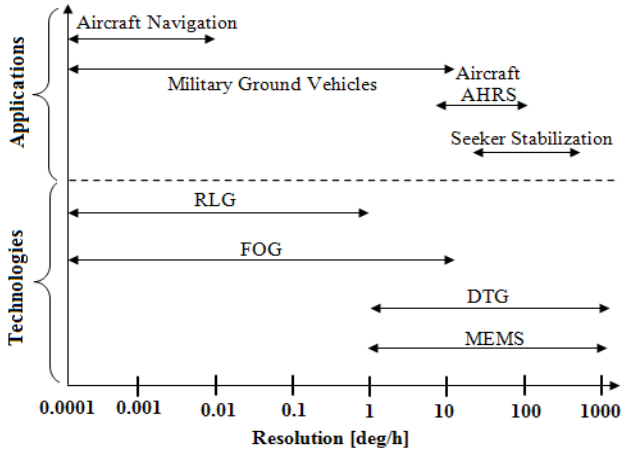

Figure 1. Comparison of Gyroscope Technologies and applications (MEMS,DTG,FOG,RLG,AHRS).

is limited by frequency of backscattering noise[3]. Interferometric Fiber-Optic Gyro (IFOG) is most recent emerging technology; the closed optical path is developed by a multi-turn optical fiber coil wound on a coil. It is more compact and potentially of lower cost than the RLG. In IFOG designs are generally integrate by a light source, detector, optical coupler, power splitter, polarizer and phase modulator in discrete component form and are connected together with fiber pigtails[7].

The principle of operation in IFOG is based on the interference of light instead of that it is passed through a fiber coil which can be as long as 5 km. In case of propagation plane undergoes angular rotation, then readout the rotation induced Sagnac phase shift between two counter propagating waves in an optical closed path, which requires very high resolution and it can be achieved when the electro optic gyroscope is a highly sensitive with an optical interferometer[8].

Various techniques employed by the modern IFOG, including optical reciprocity intended to minimize the errors on gyro performance. The performance of a gyro is mainly characterized by bias stability, scale factor linearity and stability[9]. Interferometric Fiber Optic Gyros (IFOGs) can be configured as either open loop (direct measurement) or closed loop (using feedback loop to nullify the rotation-induced Sagnac phase error), but due to its complexity restricts it presently in Avionics and Inertial Navigation Grade applications[9]. Since the output of the interferometer is characterized by a cosine function, a phase change of 2π results is no change in the output.

2. Description of Fiber Optic Gyroscope

In the field of fibre optic sensors, Fibre Optic Gyroscope (FOG) is most important development, so it has been studied and developed more than two decades[7], which senses changes in orientation, thus performing the function of a mechanical gyroscope.

Sagnac first demonstrated the optical gyroscope principle in 1913. Optical gyroscopes implemented so far use Sagnac effect (this is the physical phenomenon of an optical gyroscope operation), which states that two counter propagating beams exhibit induced optical path difference around a rotating reference frame is proportional to the absolute rotation[5]

$$\Delta\phi_s = \frac{2\pi LD}{\lambda C}\Omega$$

Where, D is diameter of the sensor coil, L is length of the optical fiber, λ is light wavelength, Ω is rotation rate and C is speed of light in vacuum.

The Sagnac interferometer operation principle is as shown in Figure 2. In case of no rotation in the system (i.e., at rest), then the propagation of light in Clockwise (CW) and counter Clockwise (CCW) directions traverse identical paths, so that, there is no phase difference between them. In case of rotation in the system with an angular rotation rate Ω, then the CW path will be longer by $\frac{LR}{C}\Omega$ and CCW path will be shorter by $\frac{LR}{C}\Omega$ and vice versa[10].

The basic configuration of FOG is as shown in Figure 3. A Super Luminescent Diode (SLD) is used as a broadband source of light and it is projected into a 3-dB optical fiber directional coupler. This coupler can be split the light into two waves. Then the two light waves propagate equally in opposite directions around the fiber coil. The interference of light waves occurred while returning to coupler and a fringe pattern is driven onto a photo detector[1].

In any two-wave interferometer, the intensity on the photo detector represents interfere of the two light waves and varies as cosine of Sagnac phase with its maximum value at zero[11]. This intensity (I or I_d) is expressed as,

$$I_d = I_0\,(1 + \cos(\Delta\phi\, s))$$

Where, I_0 is the mean value of the intensity. The detected intensity is used to calculate the rotation rate.

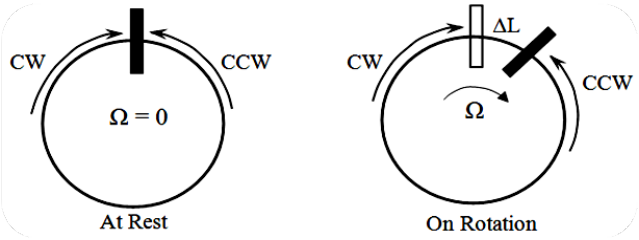

Figure 2. Sagnac interferometer working principle.

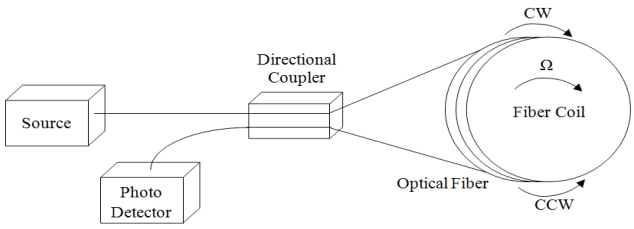

Figure 3. Basic configuration of FOG.

The limitations in the basic configuration are[5,12]: Poor sensitivity for small rotation rates, direction ambiguity, restricted dynamic range due to the 2π periodicity of the response curve and output is a nonlinear function of the rotation rate.

3. The Open Loop Configuration

In open loop approach, a lock-in-amplifier is used to measure the detector output at the fundamental modulating frequency and the rotation rate is measured directly[13]. Additionally, the amplitude of the second harmonic and the higher harmonics are also measured to suppress the variations in returning optical power and changes in the differential phase modulation voltage[14]. These changes will cause the error in the detector output, which is the major drawback in open loop design. The block diagram of an open loop fiber optic gyroscope is as shown in Figure 4[15].

When a phase modulator is used, the expression for the intensity on the photo detector is,

$$I_d = I_0(1+\cos((\Delta\phi_s)+\Delta\phi_m))$$

4. The Closed Loop Configuration

In the closed loop approach (analog) based on a sine wave biasing modulation is the interference link generates a nonlinear sine function, which confines the IFOG's dynamic measurement range. But this analog solution does not represent a very efficient solution, which is based on an analog phase ramp (also indicated as serrodyne modulation) in addition to the sinusoidal biasing modulation. Although, there is a great improvement is obtained with the digital closed-loop scheme. In this scheme, square wave biasing modulation and digital feedback phase ramp is used to reduce the closed loop error near the zero point[16] and to improve the linearity, scale factor

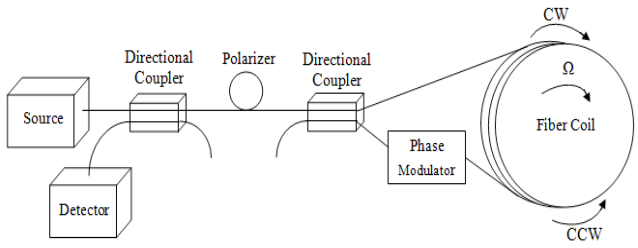

Figure 4. Open loop configuration fiber optic gyroscope with phase modulator.

stability and insensitivity against environment, especially against vibration.

In this digital approach, the phase modulator used for dynamic biasing also serves as the nonreciprocal phase shift generator. The phase modulation requires a phase modulator with laser beam to accommodate the fast reset that occurs every cycle. This necessities used of electro-optic phase modulator such as those using a channel waveguide[17].

The error signal in the output of lock-in amplifier is sampled, quantized and it is maintained, closed to zero by the digital feedback. The sampling frequency corresponds to the inverse of the radiation transit time τ, for the required synchronization of the ramp and the biasing signal[1]. It starts from the error signal and the controller is driven by the phase modulator so that it generates phase steps of amplitude equal to the Sagnac phase shift and duration τ.

The DAC automatically creates the reset of ramp signal, by means of its overflow. The reset step corresponds to a variation in a phase of 2π radian, in order to get always the correct Sagnac phase shift. In this configuration the rotation rate is achieved by direct measurement in a digital format from the error signal. Another advantage of this approach with respect to the analog solution, maintains the phase stability during the signal recovering[1].

In closed loop approach, the photo detector output demodulated at the phase modulation frequency is used as an error signal (demodulated biased signal or open-loop signal). This loop introduces a controlled amount of non reciprocal phase shift between the two counter propagating optical waves to counteract the rotation induced signal phase shift[14]. The block diagram of the closed loop configuration is shown in Figure 5[15].

Thus the net phase difference between the two interfering waves is maintained at zero regardless of the rotate rate. The amount of nonreciprocal phase shift is introduced is the output of the gyroscope and it is linearly related to the rotate rate[5,12,14] i.e., it is fed back into the system to generate an additional feedback phase difference ϕ_{fb} is maintained opposite to the Sagnac phase $\Delta\phi_s$. Therefore $\phi_{fb} = -\Delta\phi_s$

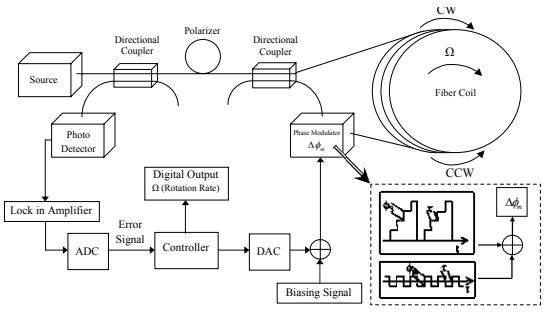

Figure 5. Schematic diagram of closed loop fiber optic gyroscope with digital phase ramp function.

5. Hardware and Software Implementation

The proposed approach is to generate the feedback signal for compensating the phase error of CLFOG system is as shown in the Figure 6. CLFOG is biased with square wave signal of period equal to transit time (τ) of the fiber-coil. Here, a square wave modulation is used to modulate the light, thereby to increase the sensitivity and to detect the rotation rate polarity. The PINFET converts optical power, which is output of FOG to electrical signal. This output is square wave modulated co-sinusoidal signal.

However, the system accepts modulated Sagnac phase error signal from the photo detector of gyro optical module (via ADC). On-board 16-bit ADC receive the data from PINFET and was processed to digitize the output with sampling frequency, which is equal to transit frequency of gyro and then performs synchronous demodulation to extract the Sagnac phase error and this error passed through a filter. The result is integrated in phase integrator with the transit time reference to get final step size. After integration process, the integrated output error signal is driven by a digital ramp generator with constant peak-to-peak amplitude (V2π) which is directly proportional to the wavelength of the source. This stair case ramp signal is used as a feedback phase

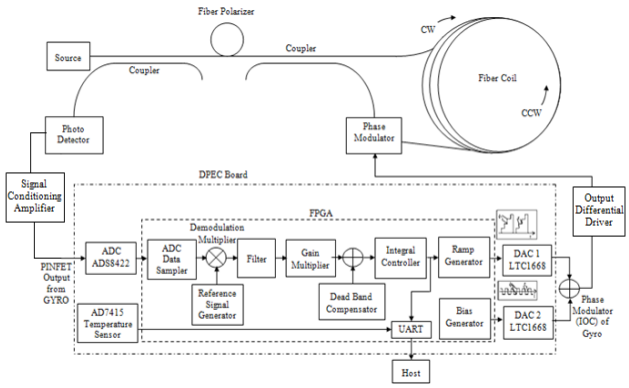

Figure 6. Proposed design approach of CLFOG.

error compensation signal to nullify the rotation induced phase shift.

Therefore, an integral controller is used with a variable gain to nullify the rotation induced Sagnac phase error of gyro with the help of a ramp generator. The feedback phase nullifying signal (ramp signal voltage is V2π and its frequency 200 KHz) and the biasing signal (square wave signal voltage is Vπ/2 and its frequency of 100 KHz) are used as control signals for CLFOG. So, the ramp signal and the square wave biasing signal for the phase modulator (IOC) of the FOG is given through 16-bit DAC.

The DPEC board transfers the phase integrator output to the host by compensating the temperature induced bias errors, upon the request of synchronization pulses. In the current design, with a selected time of every 2ms the averaged step-size data is sent to the PC.

6. Hardware Interface

In the hardware interface of the CLFOG (as shown in Figure 6), some of the components are discussed below:

6.1 ADC Interface

It is a 16-bit parallel interface used to receive data from ADC to FPGA. This data represents the modulated gyro phase error. Clock and reset to ADC is driven by FPGA. Data read synchronization control is driven by FPGA. Maximum sampling rate of ADC is 4MHz.

6.2 DAC1 and DAC2 Interface

It is also a 16-bit parallel interface used to provide data from FPGA to DAC1 and DAC2. This DAC1 data represents the square wave bias signal used for intensity modulation, whereas the DAC2 data represents the phase error compensating signal. The nature of the phase error compensating signal is stair case ramp. Clock signal to DAC is driven by FPGA. Maximum sampling rate of DAC is 20MHz.

6.3 RS232/RS422 Interface

This interface is used for Communicating with PC application software, which was implemented on UART. FPGA acting as Master of communication transfers the desired data to PC. Configuration parameters from PC are received on the serial line.

6.4 Software Interface

In software Implementation of CLFOG system, to measure the rotation rate in fiber optic gyroscope, we require some software's as follows: ProAXE SE 5.5.0, Real term serial capture program, Dev C++, Matlab program, XILINX ISE 10.1. However, the ProAXE SE software is a GUI Interface with rate table of FSPU. It is used for testing process given to our experimental setup whereas, the Real term serial capture program software is used to capture the data (hex values) from FOG and it is given to host through a MOXA Uport adapter.

7. Test Procedure

The FOG is subjected to various kinds of tests to certain its performance in terms of bias, scale factor, threshold and linearity. The gyro has externally available terminals for temperature sensor readout for each test and it is noted that all tests require stable temperatures to perform at thermal equilibrium. The gyro operating temperature is taken from 25°C to 40 °C.

Before going to the testing procedure and after switch ON the power supply, check whether the Gyro output (PINFET), biasing (square wave) and ramp signals outputs in the equipment are getting properly or not. Then proper fine tuning of the closed loop approach was observed by doing the process implementation as shown in Figure 7.

The gyro requires more than one input voltage. For each circuit, operating voltage and current should be specified in order to measure and record the input power required from each source.

Before starting up the test process, mount the gyro (CLFOG) in the fixture on the rate table so that the input reference axis (z-axis) is parallel to the table rotational axis, as shown in the Figure 8 test setup.

While mounting the gyro, care should be taken so that the effects of the earth's rotation rate may be taken into account. Connect the gyro to the output measuring and recording equipment. Apply power to the gyro, turn ON the rate table before setting the rate to the corresponding test and record the gyro output with respect to time. Here, the gyro output consists of raw data and the average data for corresponding rate.

8. Results and Comparisons

In the testing results, first open-loop and closed-loop configurations are demonstrated with rotations.

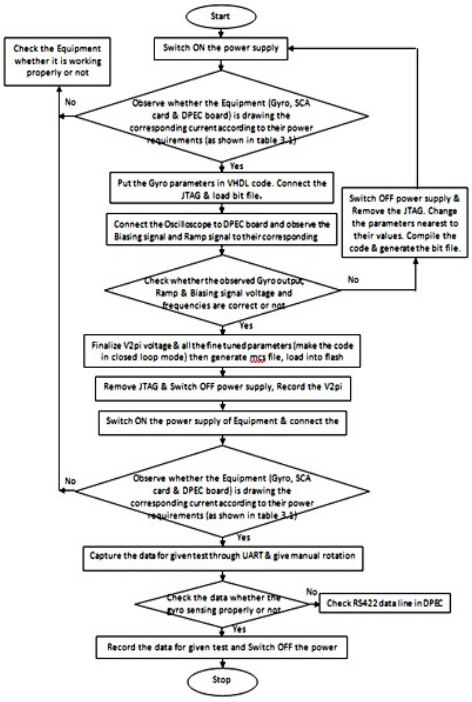

Figure 7. Process implementation for fine tuning of the closed loop approach.

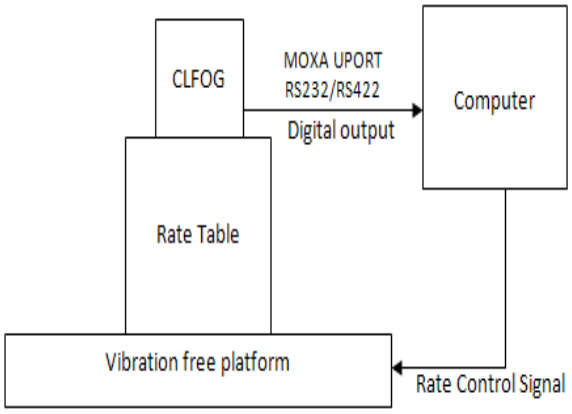

Figure 8. Test setup.

8.1 Open-loop Configuration

The output of the open loop configuration with rotation was observed in the oscilloscope as shown in the Figure 9.

In this Figure the first waveform represents the gyro output, the second represents the ramp signal and the third represents the square-wave biasing signal. In the open-loop, the amplitude of the gyro output changes with the rotation according to the square-wave biasing signal but included with the error. The ramp remains constant even with the rotation.

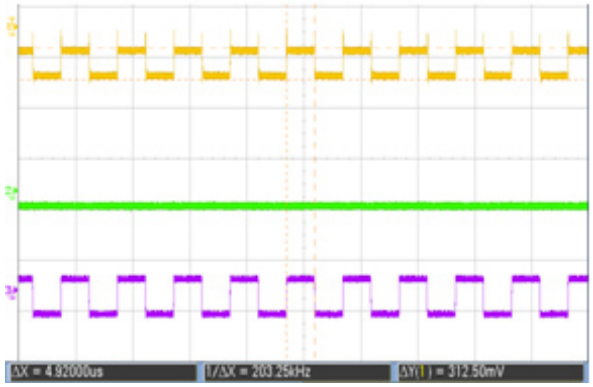

Figure 9. Output of the open loop configuration with rotation.

8.2 Closed-loop Configuration

The output of the closed loop configuration with rotation was observed in the oscilloscope as shown in the Figure 10. The feedback loop is not closed properly, so the output is changed at reset of the ramp.

To remove this error, the amplitude of the ramp voltage is adjusted to 8.75V with a frequency of 200 KHz. The gain is adjusted to compensate the error in the amplitude of the gyro output. The biasing signal is also changed according to the ramp voltage. After adjusting the amplitude of the ramp voltage, the output of closed loop configuration of proper fine tuning with rotation was observed in the oscilloscope as shown in the Figure 11

After fine tuning, the Gyro output (PINFET), biasing (square wave) and ramp signals outputs in the DPEC

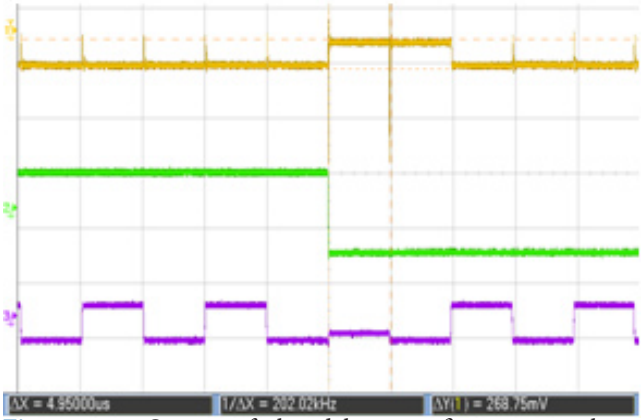

Figure 10. Output of closed loop configuration without fine tuning.

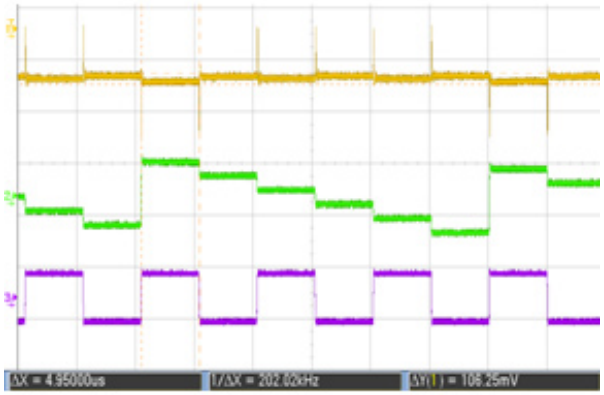

Figure 11. Output of closed loop configuration with fine tuning.

board are observed in the oscilloscope is as shown in Figures's 12, 13 and 14.

After observing the output of the closed loop configuration with proper fine tuning in the oscilloscope then the gyro was ready for the experimentation. Using this experimental setup (as shown in Figure 8) various tests are performed and their results in MATLAB are as shown in Figures's 15 to 16.

8.3 Bias

The bias test was performed for 20 minutes when V2π = 8.75V (with the fine tuning of closed loop gyro) as shown in Figure 15. In this Figure, the first waveform

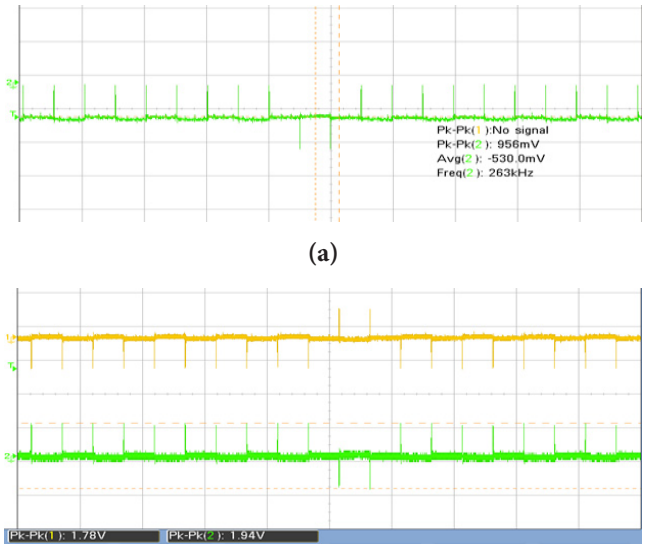

(a)

(b)

Figure 12. (a) PINFET output and (b) Differential PINFET output of a SCA amplifier before ADC.

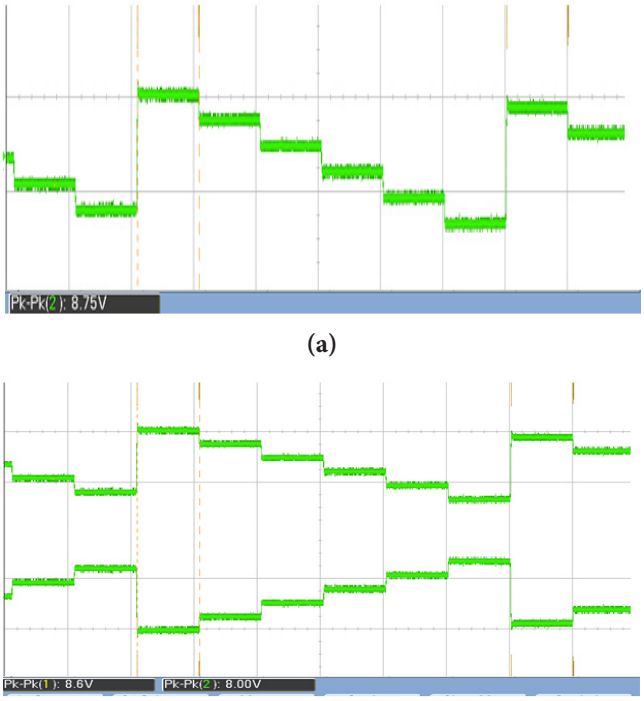

(a)

(b)

Figure 13. **(a)** Ramp Signal output at DAC 1 and **(b)** Differential Ramp Signal output at driver 1

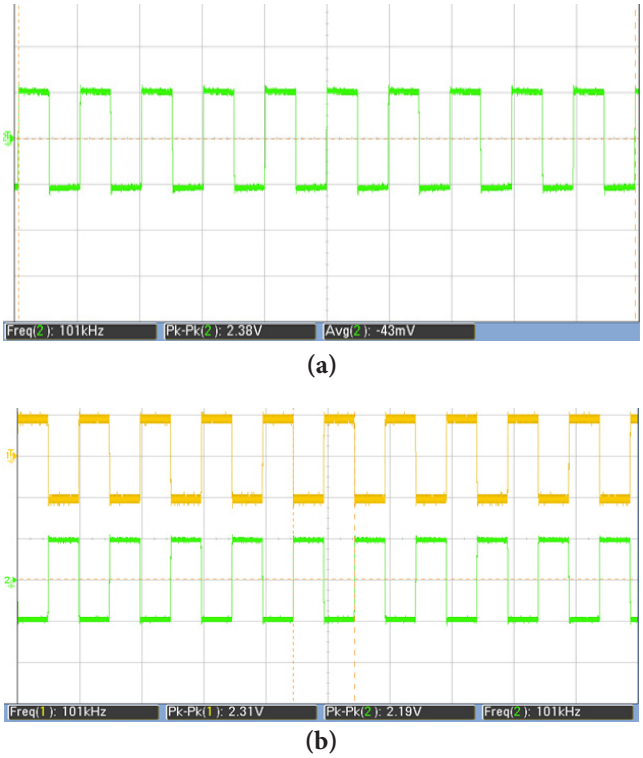

(a)

(b)

Figure 14. **(a)** Bias Signal (square wave) output at DAC 2 and **(b)** Differential Bias Signal output at driver 2

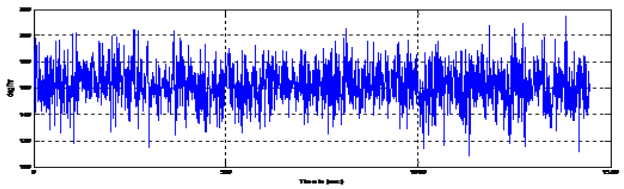

Figure 15. Bias test of the Gyro output for closed loop with fine tuning.

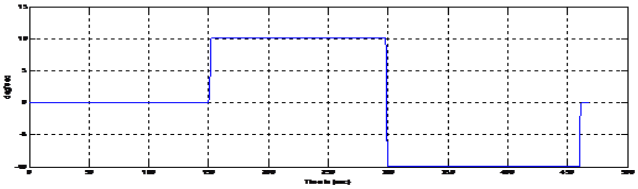

Figure 16. Scale Factor of the Gyro output for closed loop with fine tuning.

Table 1: Bias, Scale Factor and Offset Values of Closed Loop Configuration with Proper Fine Tuning

Fine Tuning	Bias (deg/hr)	Scale Factor(counts)	Offset (counts)
V2π = 8.75V	160	-2.1068375727482200E+05	4.5688664761100500E-02

represents the average data of gyro output; the second represents the corresponding average temperature data. The average data of gyro output readings is taken (as gout_avg) when the data sampling rate is 400 samples per second and obtained the bias value of 160 deg/hr and is tabulated as shown in the Table 1.

8.4 Scale Factor

The Scale Factor test is performed for 460 seconds when V2π = 8.75V (with the fine tuning of closed loop gyro) as shown in Figure 16.

In this test, positive rotation of 10deg/sec and negative rotation of –10deg/sec is given for each 2 minutes. The scale factor of 210684 counts and offset value of 0.045689 counts was calculated and it is tabulated as shown in the Table 1.

8.5 Test Results

The testing results demonstrate the bias stability, Scale Factor linearity and stability response of our proposed closed loop gyro system with proper fine tuning. The ramp voltage (or bias voltage) is increased from 1% to 10% and decreased to 1% to 10% and performed the various tests in the below three cases:

Case 1: V2π (ramp signal voltage) is varied and Vπ/2(square wave biasing signal voltage) is fixed.

Case 2: Vπ/2 (square wave biasing signal voltage) is varied and the fine tuned voltage V2πis fixed.

Case 3: BothV2π (ramp signal voltage) and Vπ/2(square wave biasing signal voltage) are varied simultaneously.

The test waveforms for each test and their tabulation are as shown below.

8.6 Bias

The bias test is performed for 20 minutes for each case. In three cases, the comparisons are made in terms of its bias values and it's tabulated as shown in the Table 2 (a, b and c).

The average data of gyro output readings is also taken (as gout_avg), when the data sampling rate is 400 samples per second, by keeping the gyro in zero seek position and the corresponding bias values for three cases are as shown in Figure 17 (a, b and c).

Table 2. Comparison for Bias Values for Three Cases

%	Bias (deg/hr)
–10%	180
–9%	190
–8%	170
–7%	180
–6%	140
–5%	160
–4%	140
–3%	150
–2%	145
–1%	145
--	160
1%	180
2%	150
3%	150
4%	140
5%	140
6%	140
7%	170
8%	155
9%	160
10%	155

(a)

%	Bias (deg/hr)
–10%	70
–9%	190
–8%	210
–7%	230
–6%	315
–5%	130
–4%	160
–3%	150
–2%	240
–1%	205
--	160
1%	180
2%	220
3%	180
4%	215
5%	215
6%	250
7%	270
8%	220
9%	90
10%	150

(b)

%	Bias (deg/hr)
–6%	100
–5%	120
–4%	40
–3%	60
–2%	130
–1%	30
--	160
1%	160
2%	160
3%	100
4%	280
5%	300
6%	250
7%	300
8%	165
9%	100
10%	300

(c)

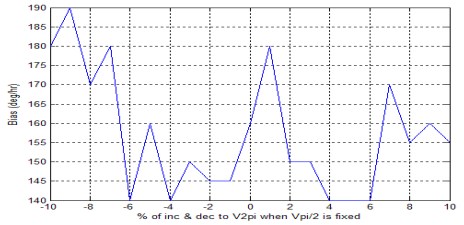

(a)

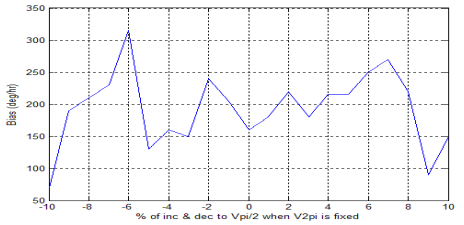

(b)

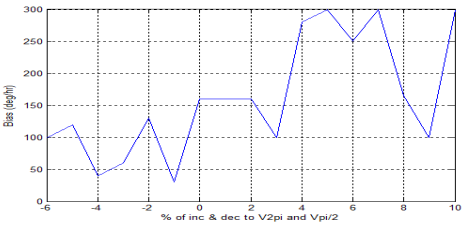

(c)

Figure 17. Comparison of bias values for three cases (a) V2π vary and Vπ/2 fixed, (b) Vπ/2 vary V2π fixed and (c) both V2π & Vπ/2 varied.

Table 3. Comparison of Scale Factor for three cases

%	Scale Factor, SF (counts)	Offset (counts)	% Change in SF
−10%	-1.755441930898760 0E+05	3.2929354077449300E-02	16.67882
−9%	-1.759433205661100 0E+05	2.5001476822680500E-02	16.48938
−8%	-1.867787644741730 0E+05	5.4979406690383900E-02	11.34639
−7%	-1.989103432214000 0E+05	5.0154895796569400E-02	5.58819
−6%	-2.016715069297500 0E+05	4.6932527850843000E-02	4.27762
−5%	-2.012885907882230 0E+05	4.0235546762655600E-02	4.45937
−4%	-2.022195703235290 0E+05	3.5618745937757200E-02	4.01748
−3%	-2.040357773865130 0E+05	4.3217157525920500E-02	3.15543
−2%	-2.064492668915280 0E+05	4.1560854406242200E-02	2.00988
−1%	-2.088305652162690 0E+05	4.2746212770939700E-02	0.87961
--	-2.106837572748220 0E+05	4.5688664761100500E-02	0.00000
1%	-2.106724269672770 0E+05	4.8489765142782900E-02	0.00538
2%	-2.150626249474200 0E+05	4.2931056692463400E-02	-2.07841
3%	-2.172200642403840 0E+05	4.2682723065092300E-02	-3.10243
4%	-2.183081565027900 0E+05	4.0261588508486400E-02	-3.61888
5%	-2.200506249607430 0E+05	3.7611691399756100E-02	-4.44594
6%	-2.216484927634290 0E+05	3.9974422778088000E-02	-5.20436
7%	-2.240826500661150 0E+05	4.5081247061905700E-02	-6.35972
8%	-2.287231944845040 0E+05	4.4384897614722000E-02	-8.56233
9%	-2.302291158131180 0E+05	4.8174477626091000E-02	-9.27711
10%	-2.287891488192150 0E+05	4.9230271854813800E-02	-8.59363

(a)

%	Scale Factor, SF (counts)	Offset (counts)	% Change in SF
-10%	-2.107564226173470 0E+05	2.1788733183813100E-02	-0.03449
-9%	-2.107488853006190 0E+05	5.2317959778610700E-02	-0.03091
-8%	-2.108096506799640 0E+05	6.6444667963387400E-02	-0.05975
-7%	-2.107088785355960 0E+05	6.3692403403481800E-02	-0.01192
-6%	-2.107853242454380 0E+05	8.7682539106047800E-02	-0.04821
-5%	-2.107798639349590 0E+05	3.5589551164846000E-02	-0.04562
-4%	-2.107891602950680 0E+05	5.1180074479956800E-02	-0.05003
-3%	-2.107656971168830 0E+05	4.3151298535416700E-02	-0.03889
-2%	-2.107113722457190 0E+05	6.7407612627303700E-02	-0.01311
-1%	-2.107321731121980 0E+05	5.6889914418962700E-02	-0.02298
--	-2.106837572748220 0E+05	4.5688664761100500E-02	0.00000
1%	-2.106722047148240 0E+05	5.2368055367527800E-02	0.00548
2%	-2.107117512787870 0E+05	6.1848205368592700E-02	-0.01329
3%	-2.107437670734730 0E+05	5.1007770404746400E-02	-0.02848
4%	-2.107771633773140 0E+05	6.1647876994825800E-02	-0.04433
5%	-2.107769230314960 0E+05	5.9275402212309200E-02	-0.04422
6%	-2.107325950457080 0E+05	6.7584434977649500E-02	-0.02318
7%	-2.107046987490230 0E+05	7.8193340563341700E-02	-0.00994
8%	-2.105926479638150 0E+05	6.2472469200708100E-02	0.04324
9%	-2.105125689733450 0E+05	2.8417034484736000E-02	0.08125
10%	-2.105270504907020 0E+05	4.4343018755010400E-02	0.07438

(b)

%	Scale Factor, SF (counts)	Offset (counts)	% Change in SF
-6%	-2.022937430847100 0E+05	1.8000244103809800E-02	3.98228
-5%	-2.138308209207310 0E+05	2.7060858317174300E-02	-1.49374
-4%	-2.047653234096530 0E+05	2.5638218517759200E-02	2.80916
-3%	-2.009022271849170 0E+05	3.8275215208675300E-02	4.64275
-2%	-2.068891623502060 0E+05	4.9435361678680600E-02	1.80109
-1%	-2.088463074876030 0E+05	2.7265256390385200E-02	0.87214
--	-2.106837572748220 0E+05	4.5688664761100500E-02	0.00000
1%	-2.129003194338840 0E+05	4.5948838414358400E-02	-1.05208
2%	-2.131908840523250 0E+05	5.2732322198344200E-02	-1.19000
3%	-2.174409946159270 0E+05	6.1751761433582000E-02	-3.20729
4%	-2.184924971112010 0E+05	6.9488050339142400E-02	-3.70638
5%	-2.195235867768590 0E+05	8.9219669216816100E-02	-4.19578
6%	-2.210871905268590 0E+05	7.2332578621132600E-02	-4.93794
7%	-2.016604864493800 0E+05	9.8878724610985400E-02	4.28285
8%	-2.248473518357140 0E+05	7.5706651451585300E-02	-6.72268
9%	-2.257212915445540 0E+05	5.3744598439323800E-02	-7.13749
10%	-2.269235712547780 0E+05	4.6844587466583200E-02	-7.70815

(c)

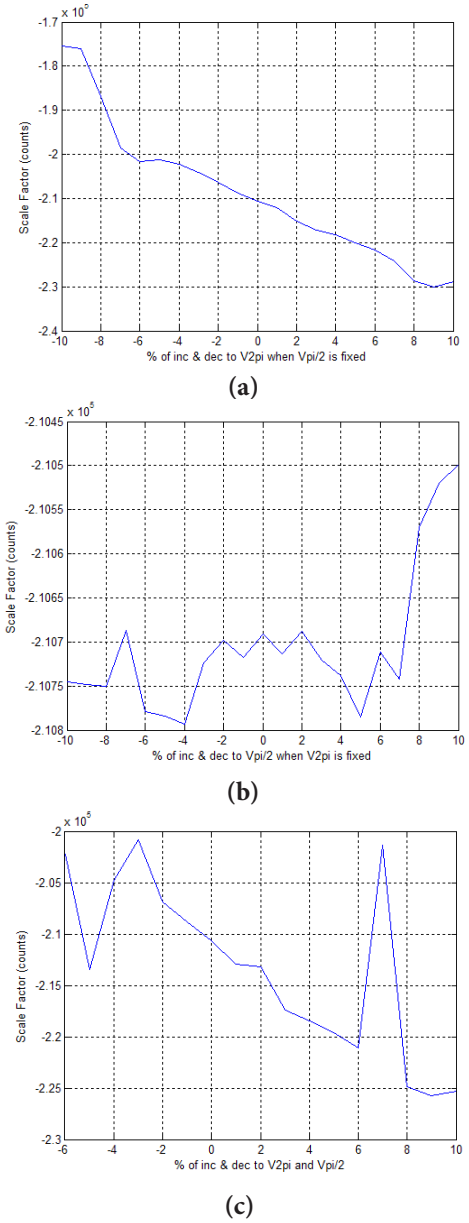

Figure 18. Comparison of Scale Factor for three cases (a) V2π vary and Vπ/2 fixed, (b) Vπ/2 vary V2π fixed and (c) both V2π & Vπ/2 varied.

8.7 Scale Factor

The Scale Factor test is performed for 300 seconds minutes for each V2π variation when Vπ/2 is fixed, similarly for each Vπ/2 variation when V2π is fixed and simultaneously for both V2π and Vπ/2 variations. In three cases, comparisons are made in terms of its scale factor and offset in counts are tabulated as shown in the Table 3 (a, b and c). It was noted that the percentage change in scale factor consists of positive and negative values i.e., it indicates that the positive for % increased and negative for % decreased.

Positive rotation of 10deg/sec and negative rotation of -10deg/sec is given and scale factor was calculated for three cases as shown in Figure 18 (a, b and c) and also the corresponding offset was calculated.

9. Conclusion

In this paper, a digital approach to derive the rotation angle in optical fiber gyroscopes (closed loop) is investigated theoretically and the performance of gyroscope is studied and the comparisons for variations in gyro parameters are made for three cases ((i) V2π (vary) and Vπ/2 (constant), (ii) Vπ/2 (vary) and V2π (constant), and (iii) both V2π and Vπ/2 are varied). From the experimental results, it was observed as follows: (i) When ramp voltage (V2π) is varying and square-wave voltage (Vπ/2) is kept constant and then the scale-factor change is increasing as the error in the signal voltage is also increases. (ii) When ramp voltage (V2π) is kept constant and biasing signal voltage (Vπ/2) is varying, the change in scale-factor is very minute and maintaining the scale-factor linearity. (iii) While varying both ramp and square-wave voltage is simultaneously, then it was observed that the device is not responding accordingly as the error is increasing. The scale-factor is out of range due to increasing the error. All these experimental results are compared with the values derived in terms of bias and scale factor. The gyro performance is very sensitive with respect to ramp voltage (V2π) variations and the percentage error is high in gyro output, but very less effect due to biasing signal voltage (Vπ/2) variations when the ramp voltage is constant. In order to avoid the bias and scale factor instabilities a proper resetting of the ramp voltage (V2π) is required.

10. Acknowledgement

The author T. Sireesha would like to express her sense of gratitude to Dr. Jagannath Nayak (SC-G), Director and G. Krishna Prasad (SC-D), Department of Inertial Systems Group, Research Center Imarat - RCI, Hyderabad, INDIA, is great-fully acknowledged for their valuable guidance and constant review in connection to completion of this project work and also express my thanks to the management of RCI for their support and encouragement during this work And also express my thanks to Dr. M. Suman, HOD of the ECM, K.L.University and also it gives me immense pleasure to thank my guide Dr .K. Sreenivasa Ravi, the faculty of Embedded Systems in K.L.University for their cooperation and help with the data collection in connection to this work.

11. References

1. Merlo S, Norgia M, Donati S. Fiber Gyroscope Principles, Electro optics Group. In: Lopez-Higuera JM. Handbook of Fibre Optic Sensing Technology; Italy: University of Pavia; John Wiley & Sons Ltd; 2000. p. 1–23.
2. Lee B. Review of the present status of optical fiber sensors. Optical Fiber Technology. 2003; 9(2):57–79.
3. Nasiri-Avanaki, MZ, Soleimani V, Mazrae-Khoshki R. Comparative assessment on the performance of open-loop and closed-loop IFOGS. Optics and Photonics Journal. 2012 Mar; 2(1):17–29.
4. Nayak J. Fiber-optic gyroscopes: from design to production. Applied Optics. 2011 Aug; 50(25):E152–E61.
5. Prasad GJ, Nayak J, Design, fabrication and testing of digital signal processing scheme for inertial grade Fiber Optic Gyroscope (FOG). Hyderabad: Inertial System Group, Research Center Imarath, RCI; 2011. p. 10.
6. Hong G, Huan Y, Wang A, Luan J. Real-time dynamic simulation of angular velocity and suppression of dead zone in IFOG. Optical Review. 2015 Feb; 22(1):39–45.
7. Ashley PR, Temmen MG, Sanghadasa M, Dutta NK, Herrick RW, Linden KJ. Test and measurement applications of optoelectronic devices. McGraw DJ; s2002.
8. Li H, Cui L, Lin Z, Zhang C. Analysis and optimization of dynamic measurement precision of fiber optic gyroscope. Mathematical Problems in Engineering. 2013; 2013: 265895.
9. Bennett SM, Emge S, Dyott RB. Fiber optic gyroscope for vehicular use, IEEEJ Our Light Tach. 1997 Nov 9-12. p. 1053–7.
10. Chunduru, Vardhani, R. Vara Lakshmi, Dhanunjay, Karthik, Greiner CM. Integrated optics devices materials and technologies. Proceedings of SPIE XIV. 2010.
11. Paul R. Fiber optic gyroscope sensors. Optical Science and Engineering. 2008:334–64.
12. Nayak J. Rajulapati RM. Modeling and simulation of signal processing for a closedloop fiber optic Gyro's using FPGA. International Journal of Engineering Science & Technology. 2012; 4(3):947–59.
13. Khan IMH. Open-loop fiber-optic gyroscope - a technical note. Defence Sciencece Journal. 1996 Oct; 46(4) 283–8.
14. Sun QD, Zhu ZH, Larouche BP. FPGA-based hardware design of closed loop control for fiber optic gyroscope. Journal of Theoretical and Applied Information Technology. 2013 May; 51(1):121–8.
15. Shiqin Z, Wu Y, Xia L, Li RL, Shang QL, Li H, Chen CH, Jang ZB, Fiber optic gyros. 20th Anniversary Conference; 1996.
16. Basak SMS. Simulation on interferometric fiber optic gyroscopewith amplified optical feedback. 2003 Sep; 87.
17. Vukmirica V. Interferometric fiber optic gyroscope: principle of operation and basic parameters determination. Scientific Technical Review. 2008; LVIII(3–4):83–91.